



Trans. Nonferrous Met. Soc. China 33(2023) 3825-3834

Transactions of Nonferrous Metals Society of China

www.tnmsc.cn



# Flotation performance and adsorption mechanism of 5-hydroxyoctan-4-one oxime to malachite

Fang-xu LI<sup>1,2,3</sup>, Ri-xiao LIN<sup>1,2,3</sup>, Gang ZHAO<sup>4</sup>

- 1. Institute of Resources Utilization and Rare Earth Development, Guangdong Academy of Sciences, Guangzhou 510650, China;
- 2. State Key Laboratory of Rare Metals Separation and Comprehensive Utilization, Guangzhou 510650, China;
- Guangdong Provincial Key Laboratory of Development and Comprehensive Utilization of Mineral Resources, Guangzhou 510650, China;
  - 4. School of Chemistry and Chemical Engineering, Central South University, Changsha 410083, China

Received 29 May 2022; accepted 10 November 2022

**Abstract:** In order to improve the utilization efficiency of copper oxide mineral resources, a novel collector, 5-hydroxyoctan-4-one oxime (HOO), was synthesized from a commodity chemical butyraldehyde and hydroxylamine hydrochloride. Its flotation performance and adsorption mechanism to malachite were investigated by flotation tests, Fourier transform infrared spectrum (FTIR), X-ray photoelectron spectroscopy (XPS) analysis and density functional theory (DFT) calculation. Flotation results of malachite showed that HOO exhibited better collecting ability and less dosage compared to benzohydroxamic acid (BHA). FTIR and XPS data gave clear evidence for the formation of Cu-oxime complex (five-membered and six-membered ring chelates) on malachite surfaces after HOO adsorption through the linkage among C—OH, C—NOH and Cu species. Moreover, DFT results showed that HOO coordinated with Cu atoms preferably through the oxime and hydroxyl groups to form bidentate chelates.

Key words: flotation; adsorption; oxime collector; copper oxide ore; malachite

# 1 Introduction

Copper is one of the important materials for the development of national economy and is widely used in various fields [1]. The rapid consumption of copper metal has led to the over-exploitation of high-quality copper sulfide resources. In order to ensure the safe use of copper, an alternative method is finding other oxide copper minerals for a supplement. Malachite is a significant oxide copper mineral found in the oxidized area of copper bearing ores [2]. Due to the uneven distribution, fine particle size, high mud content and many associated useful components, copper oxide is usually difficult to be separated [3,4]. In industry,

many mines use chemical beneficiation methods to process this type of copper oxide ore including heap leaching. Unfortunately, those methods have disadvantages such as unsatisfactory leaching rate, high consumption of chemicals, long treatment cycles and serious environmental pollution [5,6].

Flotation is the most common mineral processing method to recover copper oxide ores [7,8], and collector plays a key role in the flotation. The main function of collector is to create a hydrophobic surface on minerals. Depending on the reaction characteristics of the collector itself, there are great differences in the treatment of minerals during flotation. When using xanthate as collector, sulfurizing agents had to be used to the active copper oxide minerals surface [9–11]. Sulphidization

pretreatment is difficult to be controlled and excessive sulfurizing agents have negative effects on the flotation of copper oxide. Meanwhile, the application of alkyl hydroxamates would enable the sulphidization unnecessary due to the selective chelating ability towards copper oxide ores; however, the collecting ability was still not satisfactory [12–14]. Other collectors, such as oleic acid and amines, showed strong capture capacity for copper oxide and also enabled non-sulfidation flotation but exhibited lack of selectivity [15,16].

Similar to the hydroxamic acids, oxime compounds have been accepted as potential chelating reagents in mineral engineering. Salicylaldoxime,  $\alpha$ -benzoinoxime, 2-hydroxy-5-nonylphenyl(phenyl) methanone oxime, 2-hydroxy-1-naphthaldehyde oxime, tert-butyl salicylaldoxime and 1-(2-hydroxyphenyl)hex-2-en-1-one oxime have been proven to have a good collecting ability for malachite or other oxide ores [17–22]. The traditional view is that the phenolic hydroxyl groups in aromatic hydroxime compounds are more acidic and easier to ionize in an alkaline environment compared with straightchain hydroxime compounds. The hydroxyl groups of aromatic hydroxime (AHO) compounds are believed to be more active and easier to form bidentate chelates with transition metals [23,24]. To date, saturated hydroxyoximes (SHO) have not received enough attention in the collector development [25]. Moreover, the flotation performance of a collector is not solely determined by the chelating groups. Hydrophobic groups also play an important role in flotation bubbles [26]. Moreover, the hydrophobic value of linear alkanes as hydrophobic chains is much higher than that of aromatic compounds, which means that SHO probably has stronger collecting ability than AHO considering the collector hydrophobicity. As one of the saturated hydroxyoximes, 5-hydroxyoctan-4one oxime (HOO) has been not yet reported in public literature, especially as flotation collector for malachite.

In this work, HOO was introduced as collector for the malachite flotation, and its flotation performance was compared with that of the classic benzohydroxamic acid (BHA). Moreover, the adsorption mechanism of collectors on malachite was investigated by XPS, FTIR analysis and DFT calculation.

# 2 Experimental

#### 2.1 Materials

Natural malachite sample used in the present study was obtained from China. The X-ray diffraction (XRD) analysis of the sample showed that most of minerals were pure and suitable for single mineral flotation, as illustrated in Fig. 1. Because the recovery of malachite with small particle size is poor, the fraction with a particle size less than 37 µm was selected as single mineral flotation tests. For FTIR and XPS measurements, the finer malachite samples less than 5 µm were used. HOO was synthesized based on Scheme 1 in our laboratory with a purity of 96.5%. BHA was prepared according Song's method [27]. Other chemicals employed in the experiment were of analytical grade. All of the experiments were carried out with distilled water.

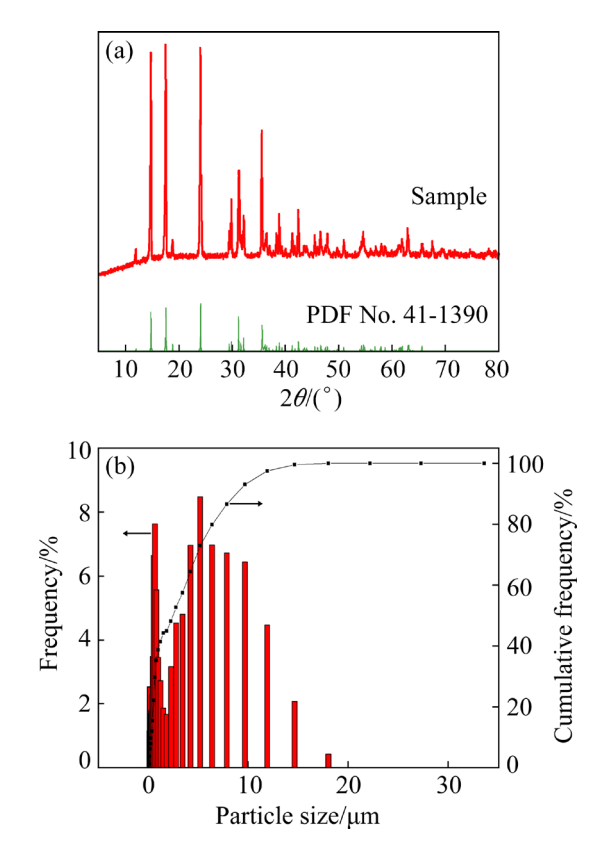


Fig. 1 XRD pattern (a) and particle size distribution (b) of malachite sample

#### 2.2 Flotation experiments

An XFG- $C_{\rm II}$  flotation machine with a 40 mL cell was used for the micro-flotation experiments. In each test, 2.00 g malachite single mineral was

$$C_3H_7$$
  $H$   $C_3H_7$   $H$   $C_3H_7$   $H$   $C_3H_7$   $C_3H_7$ 

Scheme 1 Synthetic route of HOO

dispersed in distilled water before adjusting pulp pH with 1 wt.% NaOH or H<sub>2</sub>SO<sub>4</sub> solution, and then the collector was added in the flotation cell. For BHA used as the collector, methyl isobutyl carbinol (MIBC) should be introduced as the frother, otherwise the malachite recovery was extremely low. After that, the flotation was conducted for 4 min. The floated and unfloated minerals were separately filtered, dried and weighed to calculate the flotation recovery of malachite.

The batch-flotation tests were carried out using an XFG-IV flotation machine with a 500 mL flotation cell. The copper oxide ore was ground to be less than 74 μm (>70%) in an XMB-70 rod mill. The pulp pH was adjusted to 9.0, then 200 g/t Na<sub>2</sub>SiO<sub>3</sub> and 400 g/t collector were added, and the pulp was conditioned for 2 min before flotation for 4 min. The concentrates and tailings were filtrated, dried and weighed, respectively, and the grade of Cu was determined by chemical analysis.

#### 2.3 FTIR spectrum measurements

HOO ethanol solutions were mixed with mineral samples or Cu(II) aqueous solutions at (298±1) K, respectively. After 30 min stirring, the solid product in the mixture was filtrated and rinsed three times, and then dried in a vacuum oven and prepared for FTIR measurements. The FTIR spectra of HOO, malachite before and after HOO adsorption, and Cu(II)–HOO complex were recorded with a resolution of 4 cm<sup>-1</sup> ranging from 4000 to 400 cm<sup>-1</sup> through KBr disks on a Nicolet model Nexus 670 instrument.

#### 2.4 X-ray photoelectron spectroscopy measurements

The XPS data of malachite, malachite before and after HPA adsorption, and Cu–HOO complex were recorded on a Thermo Scientific ESCALAB 250Xi using Al  $K_{\alpha}$  X-ray source operated at 200 W with 20 eV pass energy. The vacuum pressure was  $10^{-13}$ – $10^{-12}$  Pa. Binding energies were calibrated using characteristic carbon (C 1s, 284.8 eV). The

data were collected and processed using Thermo Scientific Avantage 4.52 software.

# 2.5 Computational methods

All the structure optimization and property computations were performed using Gaussian 09 software package. The molecular structures of HOO configurations were drawn in GaussView 5.0.8. The molecular geometries were pre-optimized successively by MM2 and PM6 methods, and the obtained configurations were further optimized by DFT methods. The B3LYP function with a basis set of 6-31+g\* was adopted to describe molecular structures and electronic properties. The integral equation formalism for the polarizable continuum (IEF-PCM) model was employed to optimize molecular structures and calculate molecular properties in aqueous solution. The coordination compounds of cooper ion and HOO were optimized and calculated with the same parameter setting using DFT method.

#### 3 Results and discussion

# 3.1 Preparation and characterization of HOO

HOO was prepared by using butyraldehyde and NH2OH·HCl as the starting materials. Firstly, 20.00 g butyraldehyde was added to the roundbottomed flask (100 mL) using 2.00 g Na<sub>2</sub>CO<sub>3</sub> (5 mL) and 1.00 g 3-ethyl-5-(2-hydroxethyl)-4methyl thiazolium bromide (EMTB) as the catalyst, and the mixture was stirred at 115 °C for 6 h. Next, 9.00 g NH<sub>2</sub>OH·HCl in H<sub>2</sub>O (20 mL) and ethanol (20 mL) were added to the mixture. Thereafter, NaOH was added to adjust the solution pH to 7–8, and the reaction was conditioned for 4 h at 55 °C. Finally, the light-yellow mixture was obtained after removing solvent. Product characterization: HOO, yield 76.8%. FTIR (KBr): (3361 (-OH), 2971 and 2905 ( $CH_3$ — and — $CH_2$ —), 1328, 1681 (C=N),  $1460 \, (-CH_3) \, cm^{-1}$ ; MS (ESI<sup>+</sup>): calculated for C<sub>8</sub>H<sub>17</sub>NO<sub>2</sub>, 159.13, and found 160.13 [M+H]. <sup>1</sup>H-NMR

(500 MHz, (CD<sub>3</sub>)<sub>2</sub>SO)  $\delta$ : 10.28 (s, 1H, N—OH), 3.96 (s, 1H, C—OH), 0.85 (t, 3H, CH<sub>3</sub>), 0.89 (t, 3H, CH<sub>3</sub>), 1.23 (m, 2H, CH<sub>2</sub>), 1.32 (m, 2H, CH<sub>2</sub>), 1.46 (m, 2H, CH<sub>2</sub>), and 2.25 (t, 2H, CH<sub>2</sub>); <sup>13</sup>C-HMR: 14.25, 15.34, 18.93, 19.80, 26.72, 39.72, 72.04 (C—OH), and 161.0 (C—N—OH).

#### 3.2 Flotation results

The effect of pH on flotation recovery of malachite using 1.40×10<sup>-4</sup> mol/L HOO is presented in Fig. 2(a). For HOO, it was indicated that the flotation recovery of malachite increased with increasing pH values ranging from 5 to 9 and reached 84.5% at pH 9. When the pH values were more than 9, the recovery decreased. As for BHA, the same trend on the flotation performance to malachite was shown, but the recovery was much lower compared with that of the HOO.

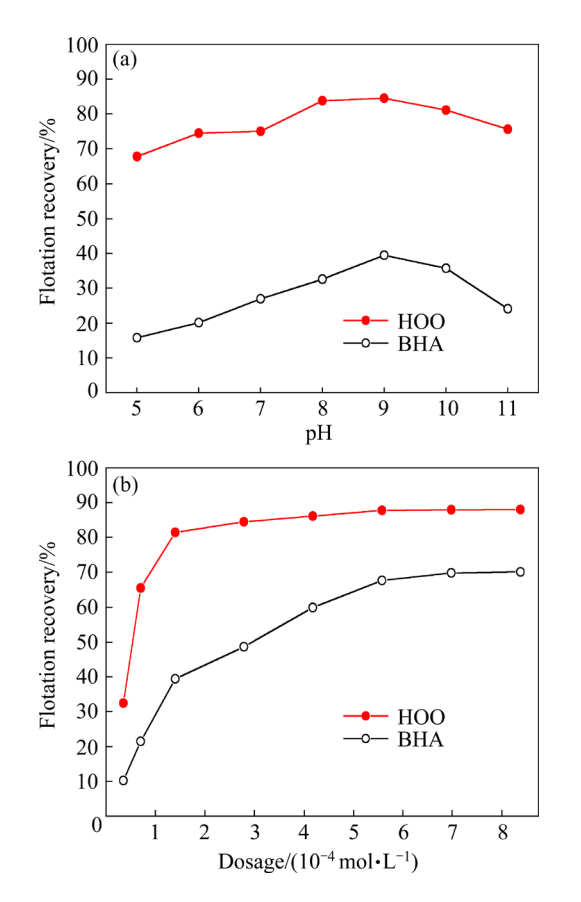


Fig. 2 Effect of pH (a) and dosage (b) on flotation recovery of malachite with HOO and BHA

The effect of HOO dosage on flotation recovery of malachite at pH 9 is shown in Fig. 2(b). For HOO, it was shown that the recovery of malachite increased rapidly with dosage ranging from  $0.35 \times 10^{-4}$  to  $2.79 \times 10^{-4}$  mol/L. When the

collector dosage was more than 4.18×10<sup>-4</sup> mol/L, the recovery increased slowly. As for BHA, it was indicated the recovery of malachite increased rapidly with the dosage ranging from  $0.35 \times 10^{-4}$  to 5.58×10<sup>-4</sup> mol/L, but the maximum recovery was also not as high as HOO. Micro flotation experiments indicated that HOO was a potential collector for malachite. The results of batch flotation are presented in Table 1, indicating that when taking HOO as the collector, the copper concentrate grade and recovery were 3.50% and 69.99%, respectively. While for BHA, the copper concentrate grade and recovery were only 3.28% and 51.28%, respectively. This indicated that reasonable modification of hydroxyl and oxime group made oximes more effective.

**Table 1** Rougher flotation results using HOO and BHA as collectors (400 g/t)

Collector	Product	Yield/%	Cu	Cu
	Troduct	11010/70	grade/%	recovery/%
	Concentrate	13.35	3.28	51.28
ВНА	Tailing	86.65	0.48	49.72
	Feed	100.00	0.86	100.00
	Concentrate	17.24	3.50	69.99
НОО	Tailing	82.76	0.31	30.01
	Feed	100.00	0.85	100.00

# 3.3 FTIR and XPS analysis results

The FTIR results of HOO, Cu(II)-HOO complex, malachite and malachite-HOO product are shown in Fig. 3.

The characteristic peaks of HOO, which were related to -OH, C=N, benzene ring, -CH<sub>3</sub> and  $-CH_2$ — groups, were found in Fig. 3(a). The stretching vibration of - OH was found at 3344 cm<sup>-1</sup>. The vibration of -CH<sub>3</sub> and -CH<sub>2</sub>could be seen at 2964 and 2876 cm<sup>-1</sup>, respectively. And the stretching vibration of —CH<sub>3</sub> was detected at 1465 cm<sup>-1</sup>. The stretching vibration of C=N stood at 1622 cm<sup>-1</sup> [28]. As for Cu(II)-HOO complex, the peak around 3333 cm<sup>-1</sup> was due to —OH. It was clear that the peak around 3344 cm<sup>-1</sup> is weakened after reaction [29]. The peaks at 2959, 2868 and 1454 cm<sup>-1</sup> were attached to -CH<sub>3</sub> and —CH<sub>2</sub>— groups. The peak of C—N moved to lower wavenumbers (blue shift) [30]. These findings implied that there may be two chelation modes between HOO and copper ions (Scheme 2).

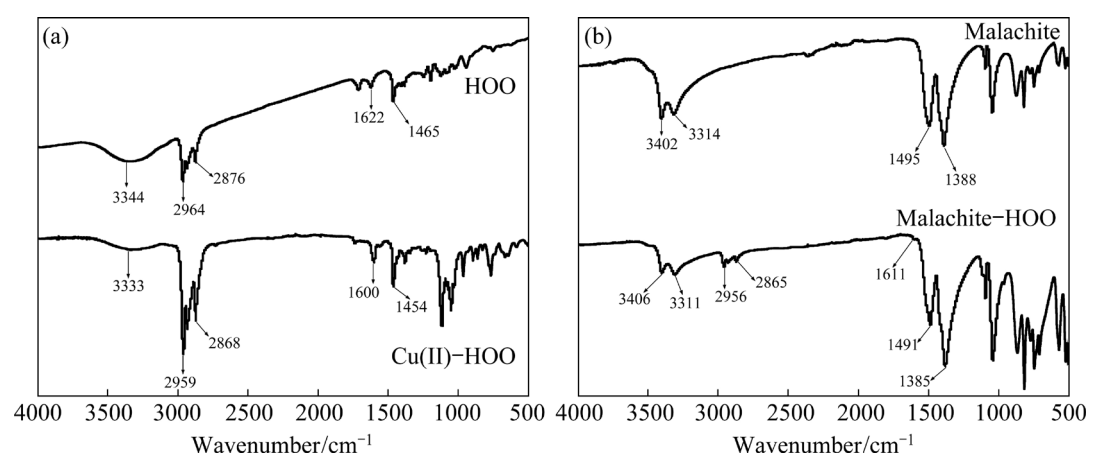


Fig. 3 FTIR spectra of HOO, Cu(II)-HOO complex (a), malachite and malachite-HOO products (b)

$$\begin{array}{c} OH \\ C_3H_7 \\ C_3H_7 \\ OH \end{array} \begin{array}{c} C_3H_7 \\ -H \text{ or } -2H \end{array} \begin{array}{c} C_3H_7 \\ + \\ N \\ OCu \\ \end{array} \begin{array}{c} C_3H_7 \\ + \\ OCu \\ \end{array}$$

Scheme 2 Possible reaction between HOO and Cu(II) ions

The chelating mode of the six-membered ring caused the —OH groups to disappear completely, while the chelating mode of the five-membered ring had one —OH group retained. This may be a reasonable explanation for the weakening rather than disappearing of the —OH group in the FTIR spectra.

The characteristic peaks of malachite were detected around 1388, 1495, 3314 and 3402 cm<sup>-1</sup>. After HOO interaction, the peaks around 2956, 2865 and 1611 cm<sup>-1</sup> were traced on the malachite surface, which was similar to FTIR spectra of Cu(II)–HOO complex. The result of malachite–HOO product showed that the peak similar to Cu(II)–HOO complex was traced on malachite after adsorption, further implying a chemisorption of HOO on malachite surface.

HOO, Cu(II)-HOO complex, malachite and HOO-malachite product were investigated by XPS. The survey and high-resolution XPS spectra of Cu, N and O are shown in Figs. 4(a, b, c, d), respectively. Figures 4(a, c) showed that N 1s peak was found on Cu(II)-HOO and malachite-HOO, while the malachite had no obvious peak without any treatment. Results of XPS analysis offered clear evidence for the adsorption of HOO on malachite. The N 1s peak indicated that numerous HOO was

fixed on mineral surface.

Figure 4(b) presented Cu 2p<sub>3/2</sub> XPS peaks of malachite, Cu(II)-HOO and malachite-HOO products. The Cu 2p<sub>3/2</sub> peak of malachite was composed of single peak. After HOO modification, The Cu 2p<sub>3/2</sub> peak of malachite was composed of three features, which appeared at 934.6, 934.4 and 932.8 eV. The Cu 2p<sub>3/2</sub> peaks of Cu(II)-HOO were centered at 934.4 and 932.8 eV. The binding energy of Cu 2p<sub>3/2</sub> of malachite-HOO product or Cu(II)-HOO complex decreased, which indicated that copper atom received electron to form electronegative HOO. And —OH and C—N—OH are the only groups in the HOO molecule with lone pair electrons. Therefore, it can be speculated that copper ions bonded with HOO through N-O-Cu and C—O—Cu linkage.

Figure 4(c) exhibited that the peaks of N 1s of Cu(II)–HOO and malachite–HOO stood at 400.6 and 400.1 eV, respectively. While for malachite, there was no signal of N peak from 369 to 405 eV. Figure 4(d) showed that the O 1s peaks of three detected objects were assigned to 533.3, 531.6 and 531.1 eV. The O 1s peak of malachite was composed of two features, which appeared at 533.3 and 531.6 eV. The O 1s peaks of Cu(II)–HOO complex were found at 533.3, 531.6 and 531.1 eV.

After HOO modification, the significant changes of O 1s at 533.3 eV on malachite surface were observed. The O 1s peak of malachite was composed of four features, which included similar O 1s peak of Cu(II)–HOO complex. The changes of O 1s XPS are important evidence showing the adsorption mechanism of HOO. There were three different types of oxygen from the O 1s spectrum of Cu(II)–HOO complex, which further verified the speculation of the infrared data. The decrease of the relative peak intensity ratio of —OH to CO<sub>3</sub><sup>-</sup> after HOO treatment indicated that the —OH groups on malachite reacted with HOO, which agreed with the finding of FTIR result.

#### 3.4 Molecular structure and theoretical studies

In order to provide further explain of adsorption model, the binding models of HOO and Cu(II) ion were calculated by DFT methods. The optimized results of HOO are given in Fig. 5. There were probably three configurations for HOO structure, and the computational energies for each configuration are also listed in Fig. 5. The relative molecular energies followed the sequence: B < C < A, which indicated that B and C configurations were more stable than A. The sequence was probably due to the intermolecular hydrogen bond for B and C configurations as shown in the molecular electrostatic potential (MEP) maps in Fig. 6.

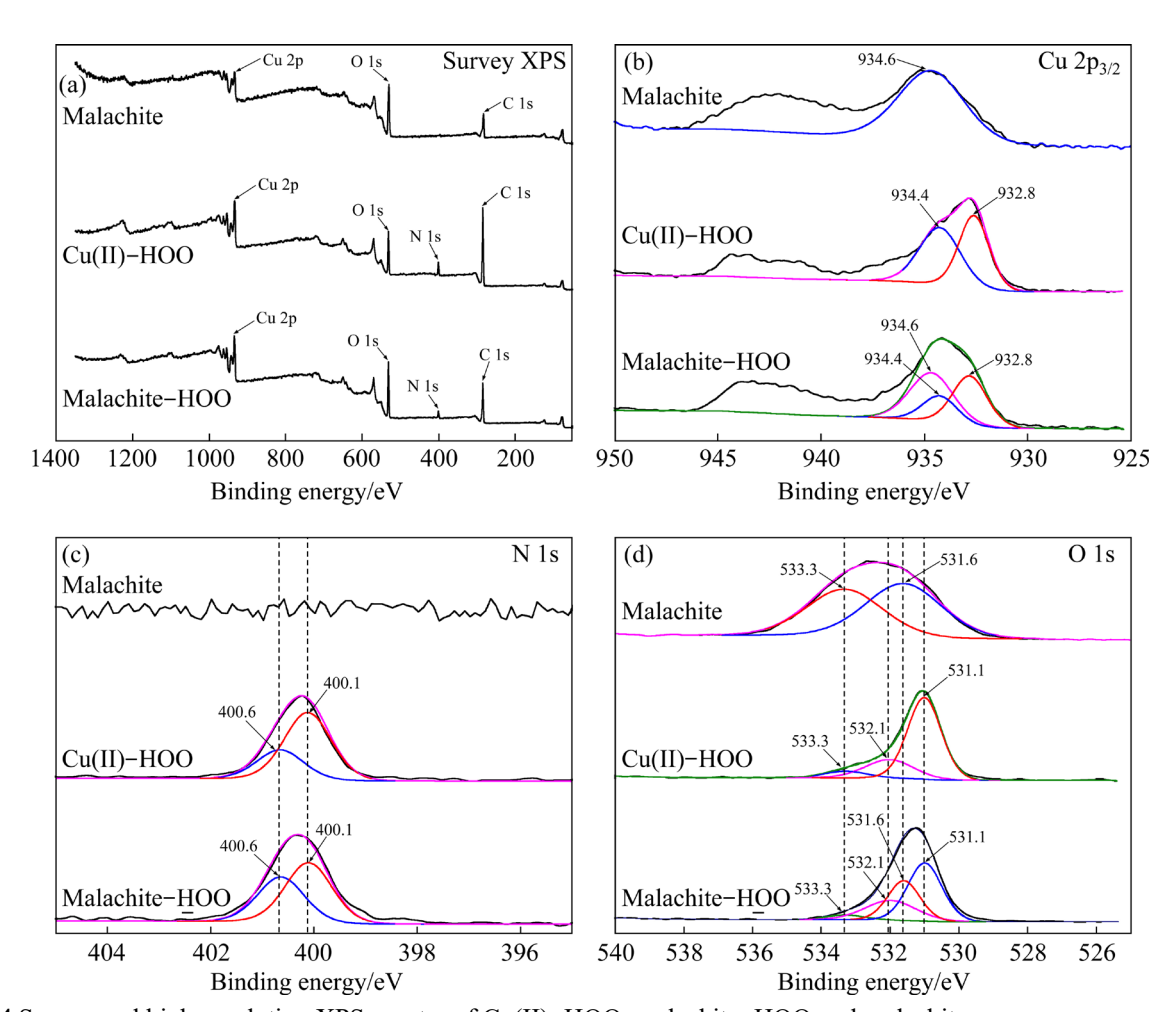


Fig. 4 Survey and high-resolution XPS spectra of Cu(II)-HOO, malachite-HOO and malachite

Fig. 5 Probable configurations for structure of HOO

The MEP maps could intuitively display the electron density and help to predict the reactive sites for electrophilic or nucleophilic attacks in various reactions [31,32]. In the majority of MEP maps, red and blue represent the regions with the most negative and the most positive electrostatic potentials, respectively. The negative charge mainly covers the O and N atoms in hydroxyl and oxime groups, respectively, while the positive charge covers the H atoms adjacent to O—N=C group. Compared with HOO molecules, the O atoms connected to the N=C groups become more negative after ionization.

The frontier molecular orbital (FMO) theory was adopted to further study the reactive center for HOO [33]. The FMO distributions for B and C configurations are shown in Fig. 7, where HOMO and LUMO represented the highest occupied molecular orbital and the lowest unoccupied molecular orbital, respectively.

The HOMOs mainly located at C—OH groups for both B and C molecules but C=N—O groups for the relative anions. As for the LUMOs, they all spread in the C—C=N—O groups for the

molecules and anions of B and C configurations. It is not difficult to find that the hydroxyl and oxime groups in HOO were the main electron donors for Cu(II)–HOO complex. In addition,  $\Delta E_{\text{LUMO-HOMO}}$  followed the order as:  $B_{\text{anion}} < C_{\text{anion}} < B_{\text{molecule}} < C_{\text{molecule}}$ . It indicated that the B configuration would be more active than C configuration, and anion configuration was the most possible form chelating copper ions than molecule configuration.

The optimized geometries for the complexes of HOO anion and Cu(II) ion are shown in Fig. 8. Five-membered and six-membered ring complexes formed through the attachment of the N and O atoms in B configuration and two O atoms in C configuration to Cu(II) species, respectively. The bond length and Wiberg bond indices of Cu—N and Cu—O are shown in Table 2, and the atom net charges in HOO anion and the complexes are shown in Table 3.

The Wiberg bond of B-Cu showed the Cu—N and Cu — O<sub>2</sub> indices were 0.210 and 0.132, respectively. And the Wiberg bond of C-Cu showed Cu—O<sub>1</sub> and Cu—O<sub>2</sub> indices were 0.215 and 0.131, respectively. The Wiberg bond indices

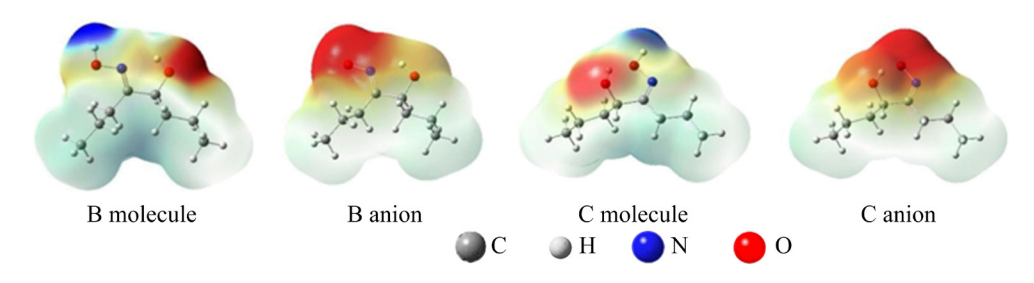


Fig. 6 MEP maps of HOO molecule and anion for B and C configurations

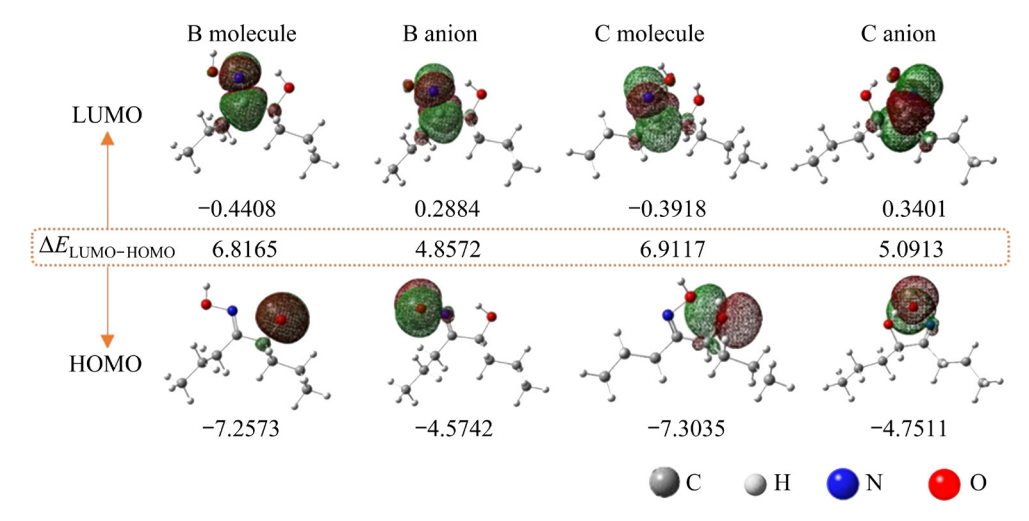


Fig. 7 Distribution and energies (eV) of HOMO and LUMO orbitals for B and C configurations ( $\Delta E = E_{\text{LUMO}} - E_{\text{HOMO}}$ )

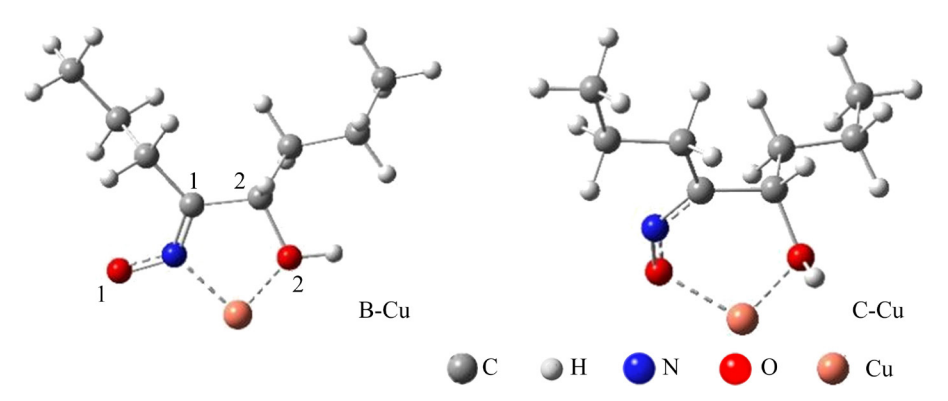


Fig. 8 Optimized geometries for complexes of B-Cu and C-Cu and selected atom labels

Table 2 Bond lengths (Å) and Cu—O/Cu—N Wiberg bond indices for HOO and complexes

		\ /				1		
Species -	Bond length				Bond length (Wiberg bond index)			
	$C_1$ — $N$	$N-O_1$	$C_1 - C_2$	$C_2 - O_2$	$O_2$ — $H$	Cu—N	$Cu-O_1$	Cu—O <sub>2</sub>
B anion	1.298	1.344	1.527	1.435	0.989	_	-	_
B-Cu	1.295	1.277	1.513	1.458	0.973	1.942(0.210)	_	2.013(0.132)
C anion	1.295	1.378	1.529	1.433	1.017	_	_	_
C-Cu	1.281	1.285	1.536	1.457	0.974	_	1.929(0.215)	2.002(0.131)

Table 3 Atom net charges in HOO anion and complexes (e)

			` /			
Species	$O_1$	N	$C_1$	$C_2$	$O_2$	Cu
B anion	-0.789	-0.212	0.100	0.053	-0.835	-
B-Cu	-0.339	-0.158	0.222	0.049	-0.829	1.078
C anion	-0.798	-0.214	0.124	0.032	-0.864	_
C-Cu	-0.484	0.034	0.186	0.041	-0.825	1.055

indicated a covalent character of the Cu—N and Cu—O bonds compared with single bond [34–36]. The bond indices of Cu—N or Cu—O<sub>1</sub> were larger than that of Cu—O<sub>2</sub>; therefore, the oxime group performed the major role in the chelation.

From Table 3, the evident transfer was observed by comparing the atom net charges in B or C anions and the complexes. The negative charges on O<sub>1</sub>, N and O<sub>2</sub> decreased both in B-Cu and C-Cu complexes, indicating the loss of electron, especially for the O atoms in the oxime groups. Consequently, similar finding could be acquired that the binding of the O—N—C group dominates in the chelation of HOO and Cu(II) species. The calculated binding energies between B or C anions and Cu(II) were -7.1650 and -7.0129 eV, respectively. These results also revealed that HOO chelated Cu(II) species mainly through the B configuration.

# **4 Conclusions**

- (1) The micro and batch flotation results indicated that HOO was a special collector for malachite flotation. Compared with classic BHA, HOO showed an excellent collecting power and less dosage for malachite. HOO provided a good demonstration of saturated hydroxime compounds in the field of copper oxide flotation.
- (2) The FTIR and XPS analysis results offered clear evidence that OH groups on malachite surface were replaced and coupled by HOO. Detailed results of FTIR and XPS implied that the —OH and OH or N in oxime groups were fixed with Cu species though C—O—Cu, N—Cu and N—O—Cu bonds, and five-membered or six-membered ring chelates formed on malachite surface. Due to the strong adsorption of HOO, the modified malachite

was recovered in flotation pulp.

(3) DFT calculations were used to explain the binding details between HOO and Cu(II) species. DFT results indicated that the hydroxyl and oxime groups in HOO were the electron donors for Cu(II)-HOO complex, and the O—N=C group dominated in the chelation of HOO and Cu(II) species. The computational results were in good agreement with FTIR and XPS analysis results.

# **Acknowledgments**

This work was financially supported by the GDAS' Project of Science and Technology Development, China (No. 2022GDASZH-2022010104). The authors are thankful for the supports from the High Performance Computing Center of Central South University, China.

#### References

- [1] WANG Lin-song, GAO Zhi-yong, TANG Hong-hu, WANG Li, HAN Hai-sheng, SUN Wei, QU Yong-bao, YANG Yue. Copper recovery from copper slags through flotation enhanced by sodium carbonate synergistic mechanical activation [J]. Journal of Environmental Chemical Engineering, 2022, 10: 107671.
- [2] XIE Tian, XU Jing-yuan, YAO Gang, ZHANG Shu-chen, TONG Xiong, QIU Guang-zhou, WANG Zhen-tang, LIU Shi-tong, SUN Xin, LIU Dian-wen, WANG Jun. Review of development status of copper-cobalt mining in Congo (DRC) [J]. The Chinese Journal of Nonferrous Metals, 2021, 31: 3422–3435. (in Chinese)
- [3] CHEN Zhi-xiang, GU Guo-hua, ZHU Ren-feng. Structural modification of cellulose to enhance the flotation efficiency of fine copper oxide ore [J]. Physicochemical Problems of Mineral Processing, 2019, 55(1): 58–69.
- [4] LI Rong-gai, SONG Xiang-yu, QIAO Jiang-hui, YU Guang-xue, LI Zhi-wei, XU Jing. Research on mineral processing technology for refractory oxidized copper ore with high mud content [J]. Mining and Metallurgical Engineering, 2008, 28(1): 46–50. (in Chinese)
- [5] TRUJILLO J Y, CISTERNAS L A, GÁLVEZ E D, MELLADO M E. Optimal design and planning of heap leaching process: Application to copper oxide leaching [J]. Chemical Engineering Research and Design, 2014, 92(2): 308–317.
- [6] LIU Mei-lin, WEN Jian-kang, TAN Gui-kuan, LIU Guo-liang, WU Biao. Experimental studies and pilot plant tests for acid leaching of low-grade copper oxide ores at the Tuwu Copper Mine [J]. Hydrometallurgy, 2016, 165(2): 227–232.
- [7] ZHANG Shi-yong, HUANG Zhi-qiang, WANG Hong-ling, LIU Ru-kuan, CHENG Chen, GUO Zhi-qun, YU Xin-yang, HE Gui-chun, FU Weng. Separation of wolframite ore by froth flotation using a novel "crab" structure sebacoyl

- hydroxamic acid collector without Pb(NO<sub>3</sub>)<sub>2</sub> activation [J]. Powder Technology, 2021, 389: 96–103.
- [8] LIU Rui-zeng, QIN Wen-qing, JIAO Feng, WANG Xing-jie, PEI Bin, YANG Yong-jun, LAI Chun-hua. Flotation separation of chalcopyrite from galena by sodium humate and ammonium persulfate [J]. Transactions of Nonferrous Metals Society of China, 2016, 26: 265–271.
- [9] CASTRO S, SOTO H, GOLDFARB J, LASKOWSKI J. Sulphidizing reactions in the flotation of oxidized copper minerals. II: Role of the adsorption and oxidation of sodium sulphide in the flotation of chrysocolla and malachite [J]. International Journal of Mineral Processing, 1974, 1(2): 151–161.
- [10] YIN Wan-zhong, SUN Qian-yu, LI Dong, TANG Yuan, FU Ya-feng, YAO Jin. Mechanism and application on sulphidizing flotation of copper oxide with combined collectors [J]. Transactions of Nonferrous Metals Society of China, 2019, 29: 178–185.
- [11] YIN Wan-zhong, SHENG Qiu-yue, MA Ying-qiang, SUN Hao-ran, YANG Bin, TANG Yuan. Effects of copper ions on malachite sulfidization flotation [J]. Physicochemical Problems of Mineral Processing, 2020, 56(2): 300–312.
- [12] FUERSTENAU M C, PETERSON H D. Flotation method for the recovery of minerals: US patents, 3438494 A [P]. 1969–04–15.
- [13] LEE K, ARCHIBALD D, MCLEAN J, REUTER M A. Flotation of mixed copper oxide and sulphide minerals with xanthate and hydroxamate collectors [J]. Minerals Engineering, 2009, 22: 395–401.
- [14] HOPE G A, BUCKLEY A N, PARKER G K, NUMPRASANTHAI A, WOODS R, MCLEAN J. The interaction of *n*-octanohydroxamate with chrysocolla and oxide copper surfaces [J]. Minerals Engineering, 2012, 36/37/38: 2–11.
- [15] LEE D H, KIM D S, LEE S H. Effect of collectors for malachite flotation from carbonate ore mixed with malachite, dolomite and calcite [J]. Journal of the Korean Society of Mineral and Energy, 2015, 52(1): 1–8.
- [16] LI Fang-xu, ZHONG Hong, XU Hai-feng, JIA Hui, LIU Gang-yi. Flotation behavior and adsorption mechanism of α-hydroxyoctyl phosphinic acid to malachite [J]. Minerals Engineering, 2015, 71: 188–193.
- [17] LI Zhi-li, RAO Feng, SONG Shao-xian, URIBE-SALAS A, LÓPEZ-VALDIVIESO A. Effects of common ions on adsorption and flotation of malachite with salicylaldoxime [J]. Colloids and Surfaces A: Physicochemical and Engineering Aspects, 2019, 577: 421–428.
- [18] UENO K, IMAMURA T, CHENG K. The handbook of organic analytical reagents [M]. 2nd ed. Boca Raton: CRC Press, 2017.
- [19] DAS B, RAVIPRASAD A. Flotation of Rakha (India) copper ore with LIX-65 NS [J]. Minerals and Metallurgical Processing, 1996, 13(2): 61–64.
- [20] XU Jin-qiu, XU Xiao-jun. Synthesis of a new collector 2-hydroxy 1-naphthaldehyde oxime and its application in rare earth ore flotation [J]. Foreign Metal Ore Dressing, 2001, 38(5): 38–39. (in Chinese)
- [21] LI Fang-xu, ZHOU Xiao-tong, LIN Ri-xiao. Flotation

- performance and adsorption mechanism of novel 1-(2-hydroxyphenyl)hex-2-en-1-one oxime flotation collector to malachite [J]. Transactions of Nonferrous Metals Society of China, 2020, 30(10): 2792–2801.
- [22] LI Li-qing, ZHAO Jing-hua, XIAO Yan-yin, HUANG Zhi-qiang, GUO Zhi-zhong, LI Fang-xu, DENG Lan-qing. Flotation performance and adsorption mechanism of malachite with tert-butylsalicylaldoxime [J]. Separation and Purification Technology, 2019, 210: 843–849.
- [23] LI Hai-hua, ZHOU Xiao-xia, YOU Zhong-lu. Synthesis, crystal structure, thermal stability, and antimicrobial activity of a hexanuclear iron(III) complex derived from 2-[1-(2-hydroxyethylimino) ethyl]phenol [J]. Chinese Journal of Inorganic Chemistry, 2013, 29(3): 649–653. (in Chinese)
- [24] SANTOS M A, MARQUES S M, CHAVES S. Hydroxypyridinones as "privileged" chelating structures for the design of medicinal drugs [J]. Coordination Chemistry Reviews, 2012, 256: 240–259.
- [25] XU Hai-feng, ZHONG Hong, WANG Shuai, NIU Ya-nan, LIU Guang-yi. Synthesis of 2-ethyl-2-hexenal oxime and its flotation performance for copper ore [J]. Minerals Engineering, 2014, 66/67/68: 173–180.
- [26] YANG Xiang-lin, BORIS A, LIU Guang-yi, ZHOU You. Structure-activity relationship of xanthates with different hydrophobic groups in the flotation of pyrite [J]. Minerals Engineering, 2018, 125: 155–164.
- [27] SONG Bao-an, LIU Xin-hua, YANG Song, HU De-yu, YU Lin-hong, ZHANG Yu-tao. Recent advance in synthesis and biological activity of oxime derivatives [J]. Chinese Journal of Inorganic Chemistry, 2005, 25(5): 507–525. (in Chinese)
- [28] XU Hai-feng, ZHONG Hong, TANG Qin, WANG Shuai, ZHAO Gang, LIU Guang-yi. A novel collector 2-ethyl-2hexenoic hydroxamic acid: Flotation performance and adsorption mechanism to ilmenite [J]. Applied Surface Science, 2015, 353: 882–889.

- [29] HARRAR-FERFERA H. Copolymerization of methyl methacrylate with 4-vinylpyridine initiated by a novel Ni(II) alpha-benzoinoxime complex [J]. Journal of Applied Polymer Science, 2010, 107(6): 3963–3973.
- [30] FANG Qi-le, CHEN Bao-liang, ZHUANG Shu-lin. Triplex blue-shifting hydrogen bonds of ClO₄···H—C in the nano-interlayer of montmorillonite complexed with cetyltrimethylammonium cation from hydrophilic to hydrophobic properties [J]. Environmental Science & Technology, 2013, 47(19): 11013−11022.
- [31] SCROCCO E, TOMASI J. Electronic molecular structure, reactivity and intermolecular forces: An euristic interpretation by means of electrostatic molecular potentials [J]. Advances in Quantum Chemistry, 1978, 11: 115–193.
- [32] LUQUE F J, LÓPEZ J M, OROZCO M. Perspective on "Electrostatic interactions of a solute with a continuum: A direct utilization of ab initio molecular potentials for the prevision of solvent effects" [J]. Theoretical Chemistry Accounts, 2000, 103: 343–345.
- [33] FUKUI K. Role of frontier orbitals in chemical reactions [J]. Science, 1982, 218: 747–754.
- [34] NACHTIGALL P, NACHTIGALLOVÁ D, SAUER J. Coordination change of Cu<sup>+</sup> sites in ZSM-5 on excitation in the triplet state: Understanding of the photoluminescence spectra [J]. The Journal of Physical Chemistry B, 2000, 104: 1738–1745.
- [35] GRZEGORZEK N, NOJMAN E, SZTERENBERG L, LATOS-GRAZYNSKI L. Copper(II) thiaethyneporphyrin and copper(II) 21-phosphoryl N-confused porphyrin hybrids: Intramolecular copper(II)—carbon interaction inside of a porphyrinoid surrounding [J]. Inorganic Chemistry, 2013, 52: 2599–2606.
- [36] BRANNAN A C, LEE Y. Photophysical tuning of σ-SiH copper-carbazolide complexes to give deep-blue emission [J]. Inorganic Chemistry, 2020, 59: 315–324.

# 5-羟基辛烷-4-酮肟对孔雀石的浮选性能及吸附机理

李方旭 1,2,3. 林日孝 1,2,3. 赵 刚 4

- 1. 广东省科学院 资源利用与稀土开发研究所,广州 510650;
- 2. 稀有金属分离与综合利用国家重点实验室,广州 510650;
- 3. 广东省矿产资源开发与综合利用重点实验室,广州 510650;
  - 4. 中南大学 化学化工学院,长沙 410083

摘 要:为提高氧化铜资源的利用效率,以丁醛和盐酸羟胺为原料合成新型捕收剂 5-羟基辛烷-4-酮肟(HOO)。通过浮选试验、傅里叶红外光谱(FTIR)、X 射线光电子能谱(XPS)分析和密度泛函理论(DFT)计算研究其浮选性能和吸附机理。浮选结果表明,与苯羟肟酸(BHA)相比,HOO 具有捕收能力强和用量低的优点。FTIR 和 XPS 的结果清楚地证明了 HOO 通过 C—OH 和 C—NOH 官能团与 Cu 原子之间键合形成铜-肟配比合物 (五元环和六元环螯合物)并吸附在孔雀石表面。此外,DFT 结果表明,HOO 能通过肟和羟基与铜原子配合形成双齿螯合物。

关键词: 浮选; 吸附; 酮肟捕收剂; 氧化铜矿; 孔雀石